



The Gut Microbiota Metabolite Succinate Promotes Adipose Tissue Browning in Crohn's Disease

Diandra Monfort-Ferré,^{a,b} Aleidis Caro,^c Margarita Menacho,^d Marc Martí,^e Beatriz Espina,^c Albert Boronat-Toscano,^{a,b} Cati Nuñez-Roa,^{a,b} Jesús Seco,^{a,b} Michelle Bautista,^d Eloy Espín,^e Ana Megía,^{a,b} Joan Vendrell,^{a,b,f} Sonia Fernández-Veledo,^{a,b}  Carolina Serena^{a,b} 

^aHospital Universitari de Tarragona Joan XXIII, Institut d'Investigació Sanitària Pere Virgili, Tarragona, Spain

^bCIBER de Diabetes y Enfermedades Metabólicas Asociadas (CIBERDEM), Instituto de Salud Carlos III, Madrid, Spain

^cColorectal Surgery Unit, Hospital Universitari Joan XXIII, 43007, Tarragona, Spain

^dDigestive Unit, Hospital Universitari Joan XXIII, 43007, Tarragona, Spain

^eColorectal Surgery Unit, General Surgery Service, Hospital Valle de Hebron, Universitat Autònoma de Barcelona, 08035, Barcelona, Spain

^fUniversitat Rovira i Virgili, Tarragona, Spain

Corresponding authors: Sonia Fernández-Veledo, PhD, Hospital Universitari de Tarragona Joan XXIII, Institut d'Investigació Sanitària Pere Virgili, Tarragona, Spain. Email: sonia.fernandezveledo@gmail.com; sonia.fernandez@iispv.cat; and Carolina Serena, PhD, Hospital Universitari de Tarragona Joan XXIII, Institut d'Investigació Sanitària Pere Virgili, Tarragona, Spain. Email: carolserena@gmail.com; carolina.serena@iispv.cat

Abstract

Background and Aims: Crohn's disease [CD] is associated with complex microbe–host interactions, involving changes in microbial communities, and gut barrier defects, leading to the translocation of microorganisms to surrounding adipose tissue [AT]. We evaluated the presence of beige AT depots in CD and questioned whether succinate and/or bacterial translocation promotes white-to-beige transition in adipocytes.

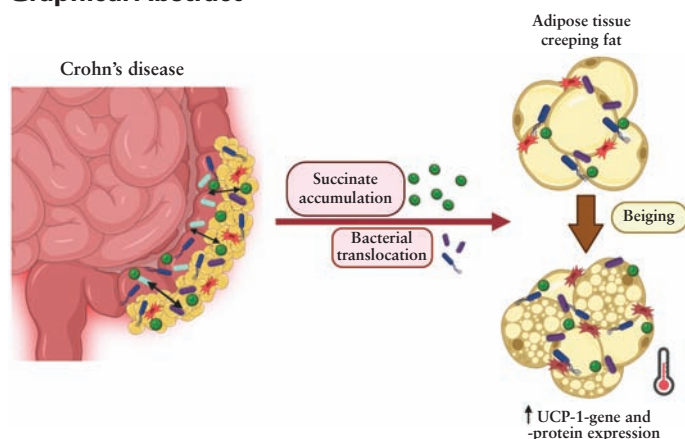
Methods: Visceral [VAT] and subcutaneous [SAT] AT biopsies, serum and plasma were obtained from patients with active [$n = 21$] or inactive [$n = 12$] CD, and from healthy controls [$n = 15$]. Adipose-derived stem cells [ASCs] and AT macrophages [ATMs] were isolated from VAT biopsies.

Results: Plasma succinate levels were significantly higher in patients with active CD than in controls and were intermediate in those with inactive disease. Plasma succinate correlated with the inflammatory marker high-sensitivity C-reactive protein. Expression of the succinate receptor *SUCNR1* was higher in VAT, ASCs and ATMs from the active CD group than from the inactive or control groups. Succinate treatment of ASCs elevated the expression of several beige AT markers from controls and from patients with inactive disease, including uncoupling protein-1 [UCP1]. Notably, beige AT markers were prominent in ASCs from patients with active CD. Secretome profiling revealed that ASCs from patients with active disease secrete beige AT-related proteins, and co-culture assays showed that bacteria also trigger the white-to-beige switch of ASCs from patients with CD. Finally, AT depots from patients with CD exhibited a conversion from white to beige AT together with high UCP1 expression, which was corroborated by *in situ* thermal imaging analysis.

Conclusions: Succinate and bacteria trigger white-to-beige AT transition in CD. Understanding the role of beige AT in CD might aid in the development of therapeutic or diagnostic interventions.

Key Words: Succinic acid; SUCNR1; beige adipose tissue; bacteria translocation, creeping fat

Graphical Abstract



1. Introduction

Crohn's disease [CD] is chronic disorder of the gastrointestinal tract characterized by severe transmural inflammation with destruction of the intestinal barrier, which increases intestinal permeability. A recent study¹ suggested that bacterial translocation across the 'leaky gut' facilitates access to the mesenteric fat and the development of an inflammatory response in the adipose tissue [AT] surrounding the damaged intestinal area, termed creeping fat.

Microbial dysbiosis in CD has been associated with an increase in succinate-producing bacteria and a decrease in succinate-consuming bacteria,² which is in good agreement with the elevated succinate levels reported in the intestine and faeces of patients with this condition.^{3–5} Classically considered as a marker of hypoxia and tissue damage, succinate is now recognized as a pro-inflammatory signal of immune activation.^{6–9} Recent observations support additional functions of succinate; for example, we and others have demonstrated that succinate serves a key role in fine-tuning the inflammatory response by acting both as an alarmin and a resolving molecule.^{10–13} Furthermore, it was reported that succinate oxidation drives AT thermogenic respiration via the production of reactive oxygen species¹⁴; the same authors later described that brown adipocytes [specialized AT cells that dissipate energy as heat] control liver extracellular succinate levels in an obesogenic environment regulated by the inner mitochondrial membrane protein uncoupling protein-1 [UCP1].¹⁵ Succinate has also been described as an inductor of brown-like adipocyte progenitors within white adipose depots [so-called brown-in-white, brite or beige adipocyte progenitors].¹⁶ In line with this latter potential function of succinate, here we hypothesized that the persistent elevated levels of succinate in areas of intestinal damage in CD would trigger *browning* of the mesenteric creeping fat by inducing the beige adipogenesis programme in adipose-derived stem cells [ASCs] as a compensatory mechanism to ameliorate inflammation and fibrosis. We further hypothesized that the presence of bacteria in the creeping fat would trigger metabolic changes in this tissue and induce browning. There is some evidence for this in the literature. Bacterial infections have been associated with an increase in pathogen-specific memory T cells,¹⁷ which respond to bacteria by secreting antimicrobial peptides¹⁸ and recruiting beige adipocytes¹⁹ in white AT. Furthermore, other infections such those produced by viruses promote beige adipogenesis in preadipocytes.^{20,21}

2. Material and Methods

2.1. Study design

Subjects were recruited at University Hospital Joan XXIII [Tarragona, Spain] and University Hospital Vall d'Hebrón [Barcelona, Spain] in accordance with the tenets of the *Helsinki Declaration*. All participants gave their informed consent, and the study was reviewed and approved by the ethics and research committees of the respective hospitals [references CEIM 177/2018; CEIM 41p/2015; PR(CS)383/2021]. Donors were classified as those in relapse [active] or in remission [inactive] following the Crohn's Disease Activity Index [CDAI] criteria and also based on biological and clinical parameters such as high-sensitivity C-reactive protein [hsCRP] and faecal calprotectin levels.

Endoscopic evaluation was performed in 80% of the patients, with complete correspondence with the clinical classification obtained by CDAI.^{22,23}

Samples of subcutaneous [SAT] and visceral [VAT, mesenteric origin] AT were obtained from patients with inactive CD [$n = 12$] and from patients without CD [control group] [$n = 15$] undergoing non-acute surgical interventions such as hernia or cholecystectomy, in a scheduled routine surgery. Samples of mesenteric perilesional [81% ileum, 5% colon and 14% ileocolon] 'wrapping' VAT [creeping fat origin] and SAT [$n = 21$] were obtained from patients with active CD scheduled for surgery for symptomatic complications or failure of medical therapy. All tissue samples were aseptically collected. Clinical data, and anthropometric, demographic and biochemical variables of the cohort are shown in [Table 1](#). Groups were matched by body mass index [BMI], gender and age.

2.2. UCP1 immunohistochemistry

Tissues were fixed in 10% neutral formalin buffer overnight, embedded in paraffin, sectioned and mounted on glass slides. The anti-UCP1 polyclonal rabbit antibody [ab10983; recommended dilution 1:500] used was purchased from Abcam.

2.3. Isolation and incubation of AT explants

VAT samples were obtained from the control group [$n = 4$] and from the active [$n = 4$] and inactive [$n = 4$] CD groups. Two fresh explants of each mesenteric VAT biopsy [~0.2 g] were placed in 1 mL of DMEM/F12 medium containing 10% fetal bovine serum [FBS]. Samples were incubated without or with succinate [250 μ M] for 24 h at 37°C and 5% CO₂.

2.4. AT-derived stem cells

ASCs were isolated as described.^{24,25} Briefly, VAT biopsies were washed extensively with PBS to remove debris and were treated with 0.1% collagenase in PBS–1% bovine serum albumin [BSA] for 1 h at 37°C with gentle agitation. Digested samples were centrifuged at 300 g at 4°C for 5 min to separate adipocytes from stromal cells. The cell pellet containing the stromal fraction was re-suspended in stromal culture medium consisting of DMEM/F12, 10% FBS and 1% antibiotic/antimycotic solution. To prevent spontaneous differentiation, primary ASC cultures at passage 0 [P0] were grown to 90% confluence and harvested with trypsin-EDTA, and aliquots [1 $\times 10^6$ cells] were cryopreserved in liquid nitrogen until required.²⁶ Adipose tissue [VAT]-derived macrophages [ATMs] were also isolated from the stromal vascular fraction of AT biopsies as described.^{24,27–29}

2.5. Adipose stem cell immunophenotyping

Cells [2 $\times 10^5$] were incubated with a panel of primary antibodies [described in [Supplementary Table 1](#)].³⁰ After isolation, the minimal functional and quantitative criteria, established by the International Society of Cell Therapy and the International Federation for Adipose Therapeutics and Science, were confirmed by flow cytometry.^{24,30} All experiments were performed in cells at P3–P5.

2.6. RNA extraction

RNA was extracted from 200 mg of AT or AT explants, or from ASCs [100 000 cells per well] using the TriPure Isolation Reagent [Roche]. RNA concentration was determined by absorbance at 260 nm, and purity was estimated with a

Table 1. Demographic characteristics and clinical data

	Control	Active CD	Inactive CD
N	15	21	12
Sex [male/female]	10/5	10/11	5/7
Age	50.8 ± 9.1	40.3 ± 12.28	46.4 ± 14.69
BMI [kg/m ²]	24.51 ± 1.9	24.49 ± 3.8	24.80 ± 7.4
Glucose [mg/dL]	81 ± 3.5	78.81 ± 17.58	84 ± 11.29
Cholesterol [mg/dL]	115 ± 15	138.4 ± 30.4	122.5 ± 17.36
HDLc [mg/dL]	38.6 ± 3.5	43.94 ± 14.45	31.13 ± 8.4
Triglycerides [mg/dL]	97.4 ± 5.9	102 ± 54.63	147.54 ± 96.6 ^a
Smoking status, <i>n</i> [%]			
Current-smoker	5 [3.3]	5 [23.8]	2 [16.6]
Never-smoker	6 [40]	14 [66]	6 [50]
Ex-smoker	4 [26.6]	2 [9.5]	4 [9.5]
Age at diagnosis, <i>n</i> [%]			
A1	—	1 [4.8]	4 [33.3]
A2	—	17 [80.9]	3 [25]
A3	—	3 [14.3]	5 [41.6]
Location, <i>n</i> [%]			
L1	—	17 [80.9]	8 [66.6]
L2	—	1 [4.8]	2 [16.6]
L3	—	3 [14.3]	2 [16.6]
Behaviour, <i>n</i> [%]			
B1	—	2 [9.5]	5 [41.6]
B2	—	9 [42.8]	4 [33.3]
B3	—	10 [47.6]	3 [25]
Corticoid treatment, <i>n</i> [%]	—	9 [52.9]	6 [50]
Biological treatment, <i>n</i> [%]	—	10 [58.8]	7 [58.3]
C-reactive protein [mg/dl]	0.15 ± 0.06	3.12 ± 0.98 ^a	0.77 ± 0.16 ^{a,b}
Faecal calprotectin [µg/g]	—	2219 ± 290.4	369.3 ± 216.5 ^b
Succinate [µM]	42.46 ± 5.06	128.82 ± 20.9 ^a	88.82 ± 10.1 ^{a,b}

Abbreviations: BMI, body mass index; HDL, high-density lipoprotein; age at diagnosis: A1 ≤ 16 years; A2 17–40 years; A3 > 40 years; location: L1 = ileal; L2 = colonic; L3 = ileocolonic; behaviour: B1 = no stenotic, no fistulizing Crohn's disease; B2 = stenotic Crohn's disease; B3 = fistulizing Crohn's disease.

^a*p* < 0.05, significant differences compared with healthy control;

^b*p* < 0.05, significant differences compared with patients with active disease.

Nanodrop spectrophotometer [Nanodrop Technologies]. cDNA was synthesized using SuperScript II reverse transcriptase and random hexamer primers [Invitrogen Life Technologies].

2.7. Real-time quantitative PCR

Quantitative gene expression was evaluated by real-time PCR [qPCR] on a 7900HT Fast Real-Time PCR System using the TaqManR Gene Expression Assay [Applied Biosystems]. Genes are listed in [Supplementary Table 2](#).

2.8. UCP1 immunofluorescence in ASCs

ASCs isolated from patients with CD were seeded at 20 000 cells/cm² and co-cultured or without bacteria and treated with succinate [250 µM] or left untreated. Cells were fixed with 4% paraformaldehyde and then permeabilized with 0.25% Triton X-100. Cells were then stained with the anti-UCP1 polyclonal rabbit antibody [dilution 1:200]. PBS was used as a negative control.

2.9. Western blotting

SAT and VAT were lysed and homogenized in M-PER buffer containing a Protease Inhibitor Cocktail, and protein concentration was determined with the BCA Protein Assay Kit [all from Pierce Biotechnology]. Equal amounts of total protein were separated by SDS-polyacrylamide gel electrophoresis, transferred to Immobilon membranes [Millipore] and blocked. Membranes were probed with polyclonal antibodies against UCP1 [Abcam], PRDM16 [ThermoFisher Scientific] and β actin [Sigma-Aldrich], which was used as a loading control. Immunoreactive bands were visualized with SuperSignal West Femto chemiluminescent substrate [Pierce Biotechnology] and images were captured using the VersaDoc imaging system and Quantity One software [BioRad].

2.10. Serum treatment of ASCs

ASCs isolated from healthy controls were seeded at 20 000 cells/cm², and serum from controls and from patients with inactive or active CD were added to cells at a 1:10 ratio [serum/

culture medium]. Cells were collected 3 h later to assess *UCP1* gene expression.

2.11. Proteomics analysis of conditioned medium from ASCs

We used an untargeted proteomics approach consisting of liquid chromatography coupled to tandem mass spectrometry to compare and identify differences in proteins secreted into the extracellular [conditioned] medium by ASCs isolated from the creeping fat of patients with active CD [$n = 9$], ASCs isolated from the VAT of patients with inactive CD [$n = 8$] and ASCs isolated from the VAT of healthy individuals [$n = 9$].

2.11.1. Sample preparation

ASCs were cultured at 94 000 cells/cm² with 0.9 mL of colourless culture medium [supplemented with 2% BSA and 1% antibiotic/antimycotic solution without FBS]. After 9 h, the conditioned medium was collected and stored at -80°C . Before analysis, 400 μL of secretome samples were concentrated to 50 μL in AmiconUltra 3 K columns [Millipore].

2.11.2. Chromatography and mass spectrometry analysis

Proteomics analysis was performed at the Centre for Genomic Regulation and University Pompeu Fabra [Barcelona, Spain] using an LTQ-Orbitrap Fusion Lumos mass spectrometer [ThermoFisher Scientific] coupled to an EASY-nLC 1200 instrument [ThermoFisher Scientific/Proxeon Biosystems] using a 90-min chromatographic gradient.

2.11.3. Data analysis

Acquired spectra were analysed using the Proteome Discoverer software suite [v2.3, ThermoFisher Scientific] and the Mascot search engine [v2.6, Matrix Science], as described.¹⁰ Proteomic data were evaluated to identify significant differences [$p < 0.05$] in proteins between the different groups. Proteins that were not present in six of the nine samples were not considered for statistical analysis. All statistical data treatments were performed with the R statistical programming environment [v3.5.3; R Core Team, 2019]. The mass spectrometry proteomics data have been deposited in ProteomeXchange with accession code PXD030520. For functional studies, STRING v11 protein–protein association networks [<https://string-db.org/>] were used to study the implicated molecular and functional pathways for the significant differentially secreted proteins.

2.12. Human ASCs co-cultured with *Escherichia coli* as an infection model

Escherichia coli [strain ATCC 25922 and an independent clinical strain] and a commensal strain of *Lactobacillus* spp. were kindly provided by Dr Terron-Puig from the Hospital laboratory of Joan XXIII of Tarragona. All three strains were cultured on agar plates and colonies were incubated at 37°C for 24–72 h. In parallel, ASCs at passage 3–5 were seeded at 60 000 cells per well in 12-well culture plates. Bacterial colonies were picked and resuspended in 2 mL PBS and the bacterial inoculum was determined by McFarland turbidity standards and counted in a Neubauer chamber. Briefly, 1×10^7 CFU/mL of bacterial suspension was centrifuged, washed and resuspended in DMEM/F12 medium without antibiotic/antimycotic solution. Subsequently, 500 μL of bacterial suspensions were added to each well with the exception of the

control wells, which received 500 μL of DMEM/F12 medium. ASCs were incubated with bacteria at 37°C for 1, 3 and 6 h [Supplementary Figure 1A]. Based on preliminary results, an incubation time of 3 h was chosen to perform the subsequent experiments. For control-ASCs, a 1-h pre-stimulus with lipopolysaccharide [LPS] at [100 ng/mL; Sigma-Aldrich] was used to mimic a pro-inflammatory condition. ASCs were then collected and used for gene expression analysis.

2.13. Succinate determination

Circulating plasma succinate levels and extracellular succinate from conditioned media of AT explants were measured with the EnzyChrom™ Succinate Assay Kit [BioAssay Systems], as described.^{10,24,31,32} The assay sensitivity was 12 μM and the intra- and interassay coefficients of variance were less than 3.5% and 6.95%, respectively.

2.14. Bio-impedance and infrared thermography

Infrared thermography and bio-impedance were performed in 12 healthy subjects, and in 11 subjects with CD [five active and six inactive], at the Hospital Universitari Joan XXIII. For infrared thermography, environmental, technical and individual factors were controlled as previously recommended,³³ and FLIR Tools was used to analyse the images [<https://www.flir.com/browse/professional-tools/thermography-software/>]. Bioelectrical impedance analysis was used to estimate body mass composition, body water volume, total energy consumption, bioelectrical phase angle and several indices of fat mass.³⁴

2.15. Statistical analysis

Statistical analysis was performed with the Statistical Package for the Social Sciences software, v15 [SPSS]. For clinical and anthropometrical variables, normally distributed data were expressed as mean \pm SD; for variables with no Gaussian distribution, values were expressed as median [25th–75th quartiles]. Student's *t*-test with Bonferroni adjustment was used to compare the mean value of normally distributed continuous variables. For variables that did not have a Gaussian distribution, we used the Kruskal–Wallis test with *post hoc* Dunn's multiple comparisons test. To analyse the differences in nominal variables between groups, we used the χ^2 test. Pearson's correlation coefficient with Bonferroni adjustment was used to analyse the relationship between parameters. For *in vitro* data, experimental results are presented as mean \pm SEM. Comparisons among the three groups were performed using the non-parametric Kruskal–Wallis test. Visualizations were performed with GraphPad Prism v6 [Graphpad Software].

3. Results

3.1. Circulating levels of succinate correlate positively with SUCNR1 expression in AT of CD patients

Plasma succinate levels were significantly higher in patients with active CD than in healthy controls [Figure 1A], in line with previous observations,^{5,35} whereas patients with inactive disease showed intermediate levels [Figure 1A]. Circulating succinate levels correlated positively with the levels of the pro-inflammatory marker hsCRP [Figure 1B].

Extracellular succinate governs local stress and inflammatory responses by binding its cognate receptor SUCNR1/GPR91,^{8,36} the expression of which is elevated in the affected

mucosa of patients with CD,³⁵ promoting pro-inflammatory and pro-fibrotic processes. Gene expression analysis of SAT samples revealed no significant changes in *SUCNR1* levels between healthy controls and patients with or without active CD [Figure 1C]. By contrast, expression analysis of samples of the surrounding VAT, in close contact with the bowel, revealed significantly higher *SUCNR1* gene expression in the VAT [creeping fat origin] from patients with active disease than from controls, and significantly lower expression in samples from patients with inactive disease [Figure 1D]. Similar results were found for ATMs and ASCs isolated from the VAT depots of the three groups [Figure 1E and F, respectively], and *SUCNR1* expression in VAT-derived ASCs correlated positively with circulating plasma levels of succinate [Figure 1G]. Given that *SUCNR1* engagement in AT is likely to modulate its inflammatory status,^{8,10,36} we treated VAT explants with succinate and surveyed the gene expression of several pro-inflammatory cytokines. Explants from patients with active disease showed a consistent increase in cytokine gene expression after the addition of succinate when compared with the other groups [Figure 1H]. Of note, the addition of succinate induced an 'anti-inflammatory' gene response in VAT samples of healthy controls, which was mimicked in VAT samples of patients with inactive disease [Figure 1H], similar to what has been reported in the SAT of healthy subjects.⁹ Succinate levels were significantly higher in the conditioned medium of AT explants isolated from patients with active CD than from patients with inactive CD and from control subjects [Figure 1I].

3.2. Adipocyte precursors from patients with CD adopt a brown-like phenotype

Because succinate is recognized as an inducer of beige adipogenesis in white adipose tissue progenitors,¹⁶ we questioned whether it could influence the characteristics of ASCs in creeping fat. We thus treated ASCs isolated from the mesenteric VAT of control and patients with CD [active and inactive] *ex vivo* with succinate and evaluated *UCP1* gene expression. We noted an increase in the expression of *UCP1* in samples from controls and from patients with inactive disease after the addition of succinate to the medium [Figure 1J]. These findings indicate that succinate probably induces browning adipogenesis in precursors both from healthy controls, as previously described,¹⁶ and also from patients with inactive CD. By contrast, succinate failed to induce *UCP1* gene expression in samples from the active disease group, which showed already high basal levels of *UCP1* [Figure 1J], probably due to exposure to an environment of elevated succinate *in vivo*. Supporting this idea, we found that the incubation of ASCs from healthy subjects with serum from patients with active CD [in whom succinate levels are higher] significantly increased *UCP1* expression [Figure 1K], and we found a positive relationship between *UCP1* expression in ASCs and circulating succinate levels [Figure 1L]. These findings suggest that ASCs isolated from patients with active CD display a brown-like phenotype with high expression of *UCP1*, and high *UCP1* gene expression is linked to high succinate levels in patients with active CD.

3.3. The brown-like phenotype of ASCs from patients with CD depends on the disease activity

To validate the browning phenotype of ASCs isolated from patients with active CD, we first tested the expression of other beige/brown adipocyte marker genes, finding a significant

increase in *UCP1*, *PRDM16*, *CPT1A*, *CPT1B*, *ELOVL3* and *ADRB3* gene expression [Figure 2A]. The expression level of several of these genes was intermediate in ASCs from patients with inactive disease except for *TBX1*, which was significantly higher in the inactive group than in the control and active groups [Figure 2A].

We next used secretome profiling to survey the proteins secreted by ASCs isolated from patients with CD [active and inactive] and from healthy controls [Figure 2B]. Network analysis of proteins secreted more in the conditioned medium of ASCs from patients revealed a significant protein-protein interaction enrichment of the network [$p < 1.0 \times 10^{-16}$] [Supplementary Figure 2]. We found a significant increase in proteins of several pathways including extracellular matrix components [POSTN, VCAN, COL12A1, LOXL2, and FBN1], and cell differentiation [Figure 2C], with several proteins related to browning including VCL, TIMP1, LTBP2, IGFBP3, IGFBP5 and FSTL1.³⁷⁻⁴⁰ The last three proteins [IGFBP3, IGFBP5, FSTL1] were lower in abundance in patients with inactive CD.^{41,42}

3.4. Bacterial colonization triggers browning in ASCs from patients with CD

Bacterial translocation from the gut to the AT is a well-recognized phenomenon in CD, prompting the growth of creeping mesenteric fat that envelops the affected intestinal wall and activates AT immune cells.¹ We recently showed that ASCs from patients with CD have unique immune properties including phagocytosis, which can be activated by bacterial signals.²⁴ We performed co-culture experiments of ASCs with a clinical *E. coli* strain to investigate whether bacteria could switch on a browning gene programme. As shown in Figure 3A, the presence of *E. coli* triggered a marked increase in *TNFA* expression in all groups of ASCs, indicating activation of the inflammatory pathway [probably to resolve the bacterial infection]. By contrast, *UCP1* gene expression was triggered only in ASCs from patients with CD [Figure 3A middle and lower panel]. This observation suggests that, in healthy conditions, a bacterial stimulus is not sufficient to trigger browning in adipocyte precursors. Furthermore, *E. coli* co-culture with ASCs from patients with active CD triggered the expression of *RAB5A* [Figure 3A middle panel], a regulator of the phagocytosis pathway.^{24,43} We repeated the experiments using a reference strain of *E. coli* [ATCC 25922] and also a commensal strain of *Lactobacillus* spp. Of note, both strains were able to increase *TNFA* gene expression but only the *E. coli* reference strain was able to significantly increase *UCP1* and *RAB5A* gene expression as compared with cells without the addition of bacteria. These findings indicate that *E. coli* strains can stimulate the beiging programme in VAT [creeping fat] of CD patients. To test the influence of a pro-inflammatory environment on ASCs, we used LPS to pre-stimulate cells from control subjects before their co-culture with *E. coli*. Results showed that an acute inflammatory stimulus was not sufficient to increase *UCP1* gene expression in control ASCs [Supplementary Figure 1C, left panel]. We repeated the experiment in ASCs from patients with active CD, finding that an acute inflammatory stimulus plus the addition of bacteria did not further increase the gene expression of *UCP1* compared with bacteria alone [Supplementary Figure 1C, right panel]. Immunofluorescence staining of *UCP1* in ASCs from patients with active CD [pre-treated or with bacteria or untreated] confirmed the gene expression findings and

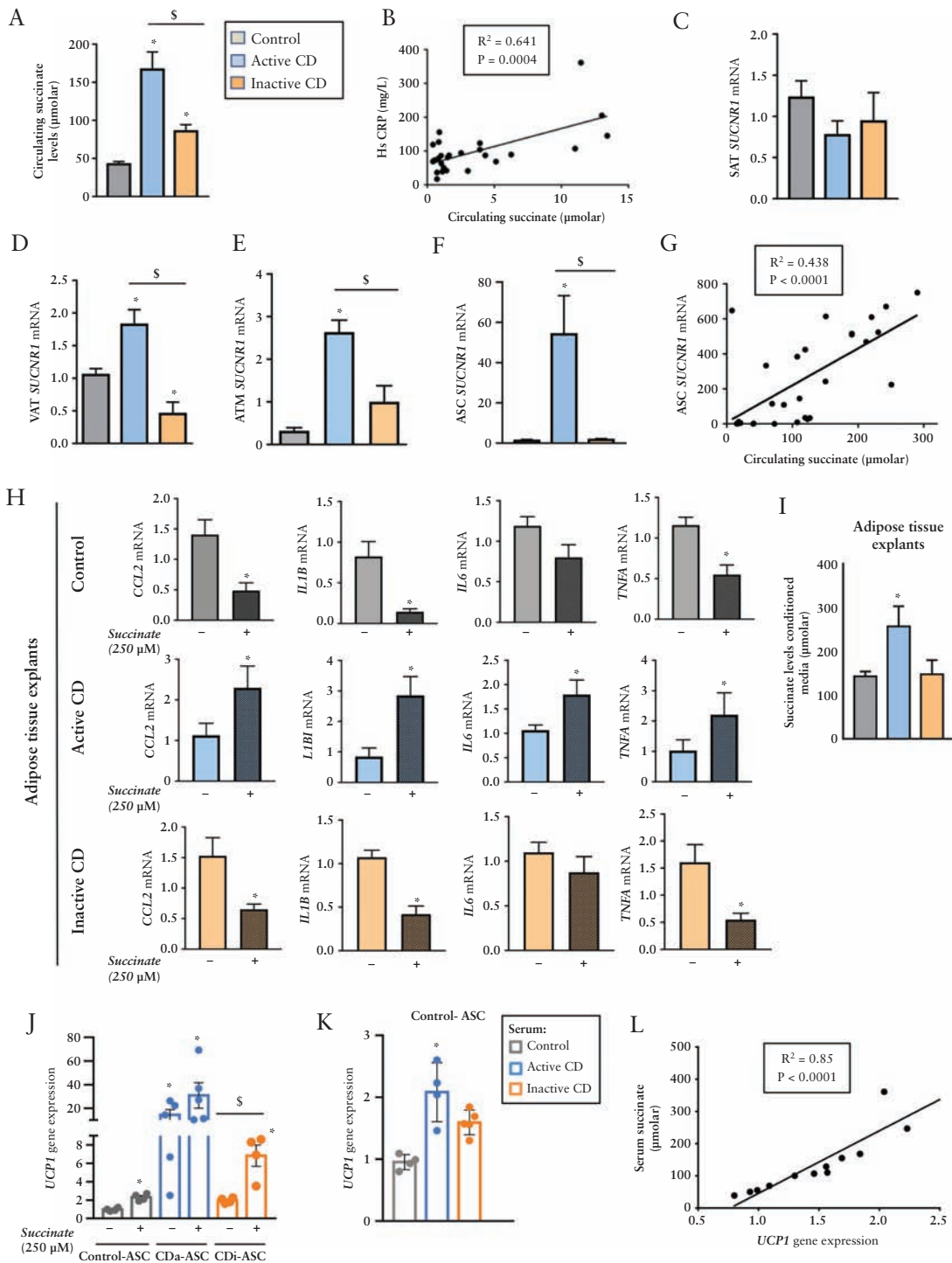


Figure 1. Succinate levels are elevated in the active phase of Crohn's disease and correlate positively with *UCP1* gene expression in pre-adipocytes. [A] Circulating succinate plasma levels in controls [healthy subjects] ($n = 10$) and in patients with active ($n = 17$) or inactive ($n = 12$) Crohn's disease [CD]. Differences were analysed with the Kruskal–Wallis test with *post hoc* Dunn's multiple comparison test. * $p < 0.0001$ vs. control; § $p < 0.05$ vs. active CD. [B] Positive correlation between plasma succinate and high-sensitivity C-reactive protein [hsCRP] levels. [C] *SUCNR1* expression in subcutaneous [SAT] and [D] visceral [VAT] adipose tissue [$n = 8$ per group], and in [E] VAT-derived adipose tissue macrophages [ATMs] [$n = 5$ per group] and [F] VAT-derived stem cells [ASCs] [$n = 8$ per group]. [G] Positive correlation between visceral-ASC *SUCNR1* mRNA and circulating succinate. [H] Succinate treatment differentially affects adipose tissue of patients with CD according to clinical status. Quantitative PCR analysis of pro-inflammatory genes in VAT explants, unstimulated or stimulated with succinate [250 µM] for 24 h, from controls and from patients with active or inactive CD [$n = 4$ per group]. [I] Succinate release in 24-h-conditioned medium of VAT explants from controls and from patients with active or inactive CD [$n = 4$ per group]. [J] *UCP1* expression in ASCs from controls and from patients with active or inactive CD after succinate treatment. [K] Serum from patients with active CD [which has a high amount of succinate] increases *UCP1* gene expression in ASCs isolated from controls. [L] Positive correlation between *UCP1* expression in ASCs and plasma succinate levels. Pearson's correlation coefficient with Bonferroni adjustment was used to analyse the relationship between parameters. * $p < 0.05$ vs. control; § $p < 0.05$ as indicated in the figure.

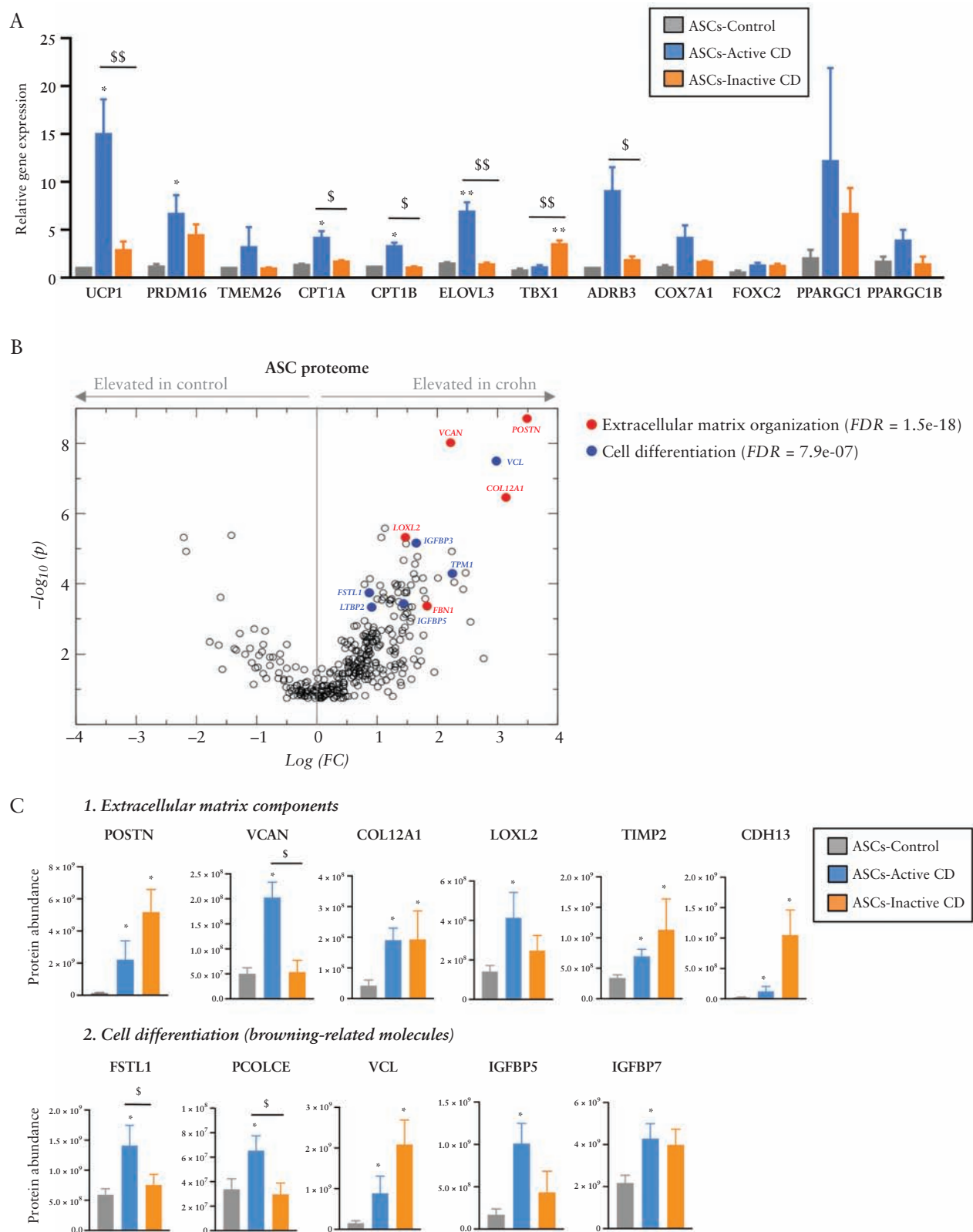


Figure 2. Adipose stem cells isolated from patients with Crohn's disease show a brown-like phenotype. [A] Relative gene expression of browning markers in adipose stem cells [ASCs] from visceral adipose tissue [VAT] of patients with active [$n = 6$] or inactive [$n = 6$] Crohn's disease [CD] or from healthy controls [$n = 3$]. [B, C] Analysis of the ASC protein secretome and protein abundance differences between ASCs of the control group [$n = 9$] and of the active [$n = 9$] and inactive [$n = 8$] CD groups. Shown are examples of enriched pathways [extracellular matrix components and cell differentiation pathways]. Bars in graphs represent mean \pm SEM. * $p < 0.05$ vs control; \$ $p < 0.05$ and \$\$ $p < 0.01$ as indicated in the figure.

revealed an enhancement of UCP1 expression after *E. coli* co-culture [Figure 3B], which was corroborated after quantification of the signal [Figure 3C].

3.5. Beige phenotype of AT in patients with CD is associated with higher body temperature

Finally, we explored whether the browning phenotype evident in adipocyte precursors obtained from the VAT of patients with CD was also detectable in whole tissue and organs. UCP1 expression was significantly higher in AT samples of patients with CD than of healthy controls, both in VAT and SAT depots, and with a clear predominance in VAT of patients with active disease [Figure 4A]. We also analysed the protein expression of UCP1 and PRDM16 in SAT and VAT depots by western blotting. Results showed that VAT UCP1 levels were significantly greater in patients with active disease [Figure 4B]. In good agreement with this, immunohistochemical analysis [Figure 4C] and quantification [Figure 4D] revealed higher UCP1 staining in both the SAT and VAT depots of patients with active or inactive disease than in healthy controls.

When we expanded the analysis to several other genes expressed in beige/brown fat cells, many of them were elevated in the VAT from patients with CD [Figure 4E], and some showed a differential behaviour depending on whether the disease was active or inactive [*ADRB3* and *COX7A1*]. Intriguingly, we found an increase of the beige cell progenitor marker *TBX1* in VAT of both active and inactive patients. An additional experiment treating ASCs isolated from active CD patients with succinate resulted in a significant increase of *TBX1* [0.81 ± 0.15 vs 3.6 ± 0.42 , $p = 0.0116$, data not shown], indicating that succinate could switch white adipocyte progenitors into beige adipocyte progenitors.

By contrast, when we repeated the analysis in SAT, with the exception of UCP1 expression only *COX7A1* was significantly higher in patients with active disease and a trend for lower gene expression was found in patients with inactive disease [Figure 4F].

Abdominal thermal imaging revealed an evident increase in the intestinal area temperature in patients with active CD [Figure 5A]. Indeed, this analysis revealed an average peak temperature of $35.76 \pm 0.49^\circ\text{C}$ for patients with active CD, $34.23 \pm 0.55^\circ\text{C}$ for patients with inactive disease and $33.88 \pm 0.78^\circ\text{C}$ for healthy controls [Figure 5B]. Notably, the minimum temperature for patients with active and inactive disease and healthy subjects was 33.68 ± 0.77 , 30.4 ± 0.60 and $30.09 \pm 0.93^\circ\text{C}$, respectively; and the average temperature was 34.66 ± 0.49 , 32.15 ± 0.61 and $30.09 \pm 1.10^\circ\text{C}$, respectively [Figure 5B]. We found no significant differences between the three groups in relation to AT indices analysed by bio-impedance [fat-free mass index, fat mass index or total VAT] [Supplementary Table 3]. As might be expected,^{44,45} a significant decrease in skeletal muscle mass and phase angle was found in patients with active disease [Supplementary Table 3].

4. Discussion

In the present study we report, for the first time to our knowledge, a browning phenotype in the creeping fat and other AT depots of patients with active CD. Creeping fat is a recognized source of adipocyte-produced soluble factors including inflammatory and anti-inflammatory cytokines;^{46,47} however, the cell types involved in anti-inflammatory responses are

unknown. It has been proposed that adipocytes from creeping fat maintain their ability to counteract inflammation and may possibly serve a protective function.⁴⁷ In this sense, the white-to-beige transition of adipocytes may explain the increase of anti-inflammatory cytokines reported in the creeping fat of patients with CD.^{46,47} Of note, our proteomics data revealed a high abundance of follistatin from CD-ASCs, which is a positive regulator of brown adipose tissue function by blocking TGF- β signalling pathways and GDF8 [myostatin] actions, and by exerting anti-inflammatory effects.^{41,48,49} Indeed, white AT precursor cells can be modified with different factors to produce AT that is more energetically active.^{50,51} Extracellular signals include activation of the sympathetic nervous system, immune cells and epigenetic changes,⁵² which influence the transcription of specific genes.⁵³ Because beige adipocytes utilize glucose, succinate and other metabolites, they essentially clear these products from the circulation, which increases glucose and insulin sensitivity.^{14,54} Accordingly, the oxidation of local and circulating succinate during browning probably reduces its levels, in turn reducing AT inflammation and fibrosis specifically in creeping fat. An important point of discussion is the origin of succinate as it could be produced both by the host and the gut microbiota. In this sense, previous studies point to gut microbiota as the main source of succinate in CD.⁵ However, it should be not ruled out that AT, the intestine and other damaged tissues may contribute to increasing succinate levels in CD patients. Further studies will be required to understand the origin of succinate levels in patients with CD.

Chouchani and colleagues recently demonstrated that UCP1⁺ adipocytes modulate liver extracellular succinate levels, and they elegantly showed that UCP1 facilitates the clearance and catabolism of circulating succinate by brown and beige AT.¹⁵ We propose that, similarly, beige adipocytes associated with CD might contribute to temper tissue fibrosis and disease pathogenesis. Fibrosis is a consequence of local chronic inflammation,⁵⁵ and strategies to promote browning of white AT to reverse fibrosis and chronic inflammation have been proposed in other inflammation-related diseases including liver steatosis⁵⁶ and may have also beneficial effects in CD.

We demonstrate that the AT of patients with active disease has a beige phenotype defined by an increase in the expression of UCP1, which is typically absent in white AT. Notably, UCP1 expression in ASCs correlates with circulating succinate levels, and it is possible that succinate regulates UCP1 in preadipocytes to prevent chronic inflammation and fibrosis, perhaps mediated by SUCNR1 signalling. However, further investigations are needed to confirm this. Intriguingly, succinate treatment increased the expression of the beige cell progenitor marker, *TBX1*, in ASCs isolated from CD subjects. Our data point to other functions of succinate apart from controlling the potential of beige adipogenesis of ASCs;⁵ succinate may also act directly in the progenitor adipocyte cell, switching white progenitor cells into beige progenitor cells, and thus limiting white adipogenesis from the beginning.

Creeping fat is an extremely complex environment, and recent studies have shown that inflammation-induced barrier dysfunction triggers bacterial translocation.^{1,57} We found that *E. coli* co-cultured with ASCs isolated from patients with CD increased UCP1 expression together with *RAB5A* gene expression, but only in ASCs from patients with active disease. This may indicate an activation of the phagocytosing ability of ASCs, which

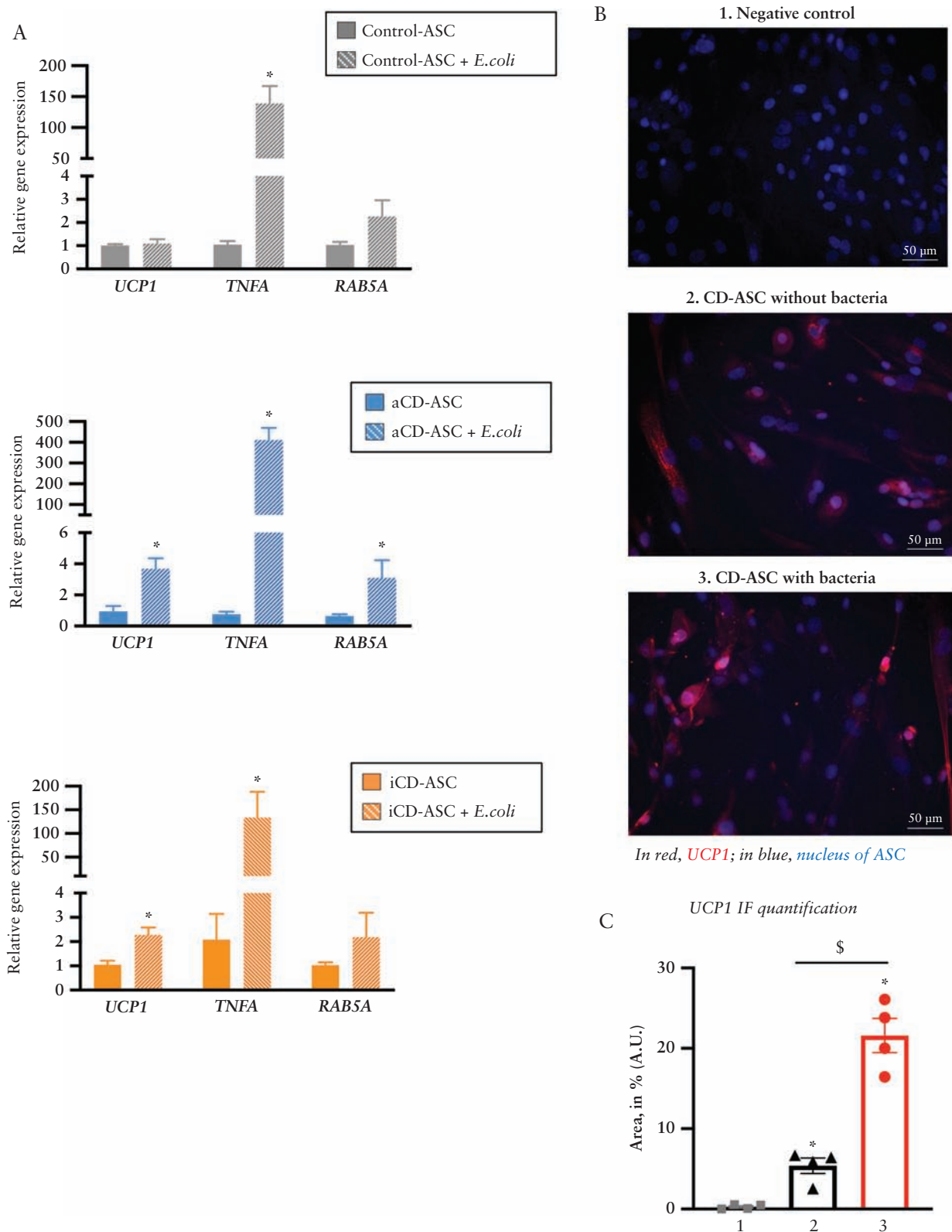


Figure 3. *E. coli* promotes browning in adipose stem cells isolated from creeping fat. [A] Relative gene expression analysis of the browning marker *UCP1*, the inflammatory marker *TNFA* and the phagocytic marker *RAB5A* in adipose stem cells [ASCs] isolated from visceral adipose tissue [VAT] of patients with active or inactive Crohn's disease [CD] or from healthy controls, co-cultured or not for 3 h with *E. coli*. Bars in graphs represent mean \pm SEM and significant differences vs cells without *E. coli* [$p < 0.05$] [$n = 3$ per group]. [B] Immunofluorescence of *UCP1* [red label] in ASCs isolated from patients with active CD co-cultured or not with *E. coli* [3 h]. DAPI staining of nuclei in blue. * $p < 0.05$ vs control [$n = 4$ per group]. [C] *UCP1* immunofluorescence quantification [% of fluorescence area, mean values \pm SEM] [$n = 4$ per group].

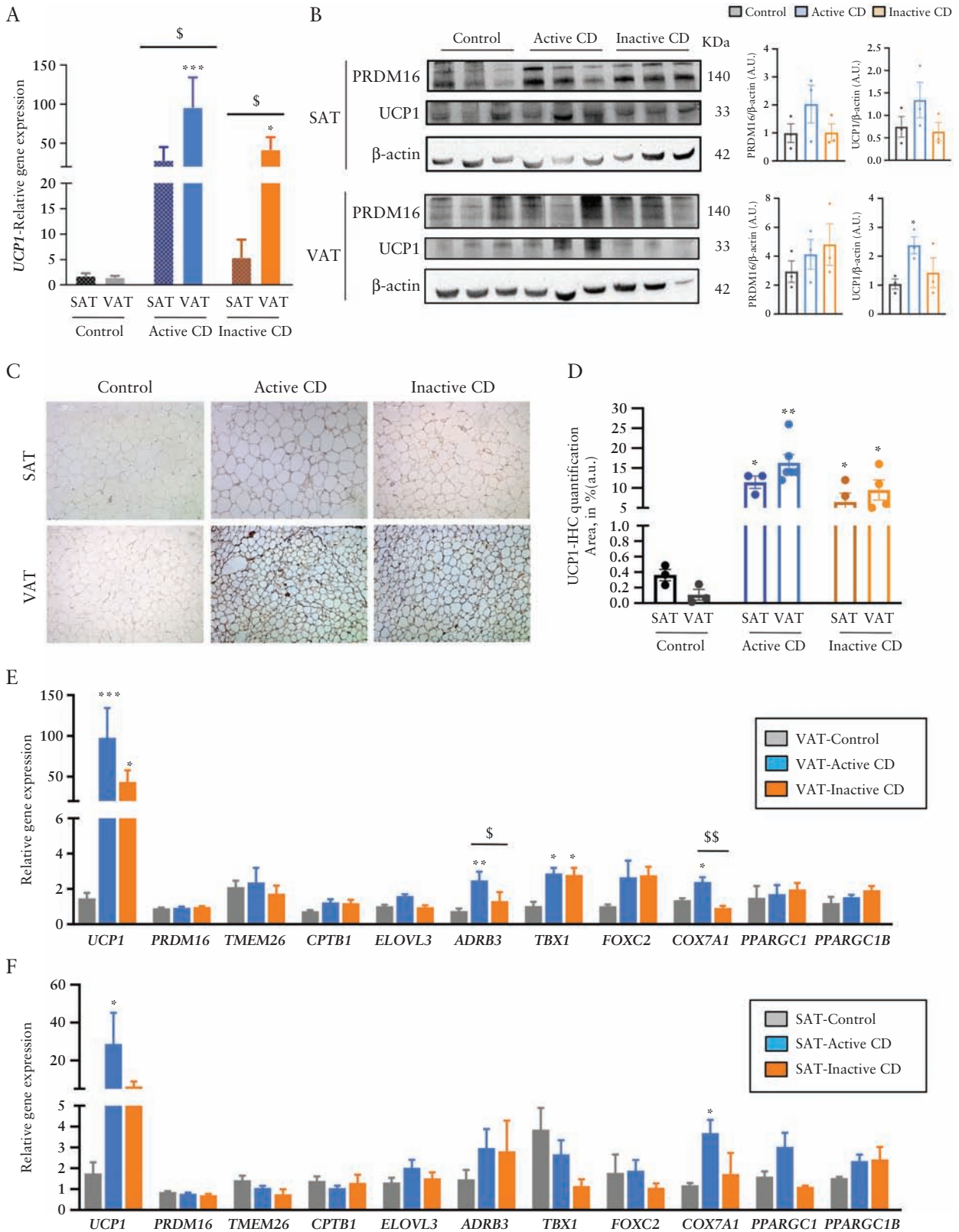


Figure 4. White-to-beige adipose tissue conversion in the subcutaneous and visceral fat depots of patients with Crohn’s disease. [A] Relative *UCP1* gene expression in subcutaneous [SAT] and visceral [VAT] adipose tissue samples of patients with active or inactive disease and in healthy individuals. [B] Western blotting of PRDM16 and UCP1; β actin was used as a loading control. Image and densitometry analysis [a.u., arbitrary units] [*n* = 3 per group]. All data are shown as mean ± SEM; **p* < 0.05 [two-tailed unpaired *t*-test]. [C] Representative immunohistochemical staining of UCP1 in SAT and VAT tissue sections of the different groups and UCP1 quantification [area in percentage of staining] [*n* = 3–6 per group]. All data are shown as mean ± SEM; **p* < 0.05 [two-tailed unpaired *t*-test]. Relative gene expression of several browning markers in [D] VAT and [E] SAT in active [*n* = 9] and inactive [*n* = 7] disease and in healthy individuals [*n* = 6]. Bars in graphs represent mean ± SEM. **p* < 0.05 vs control; §*p* < 0.05 and §§*p* < 0.01 as indicated in the figure.

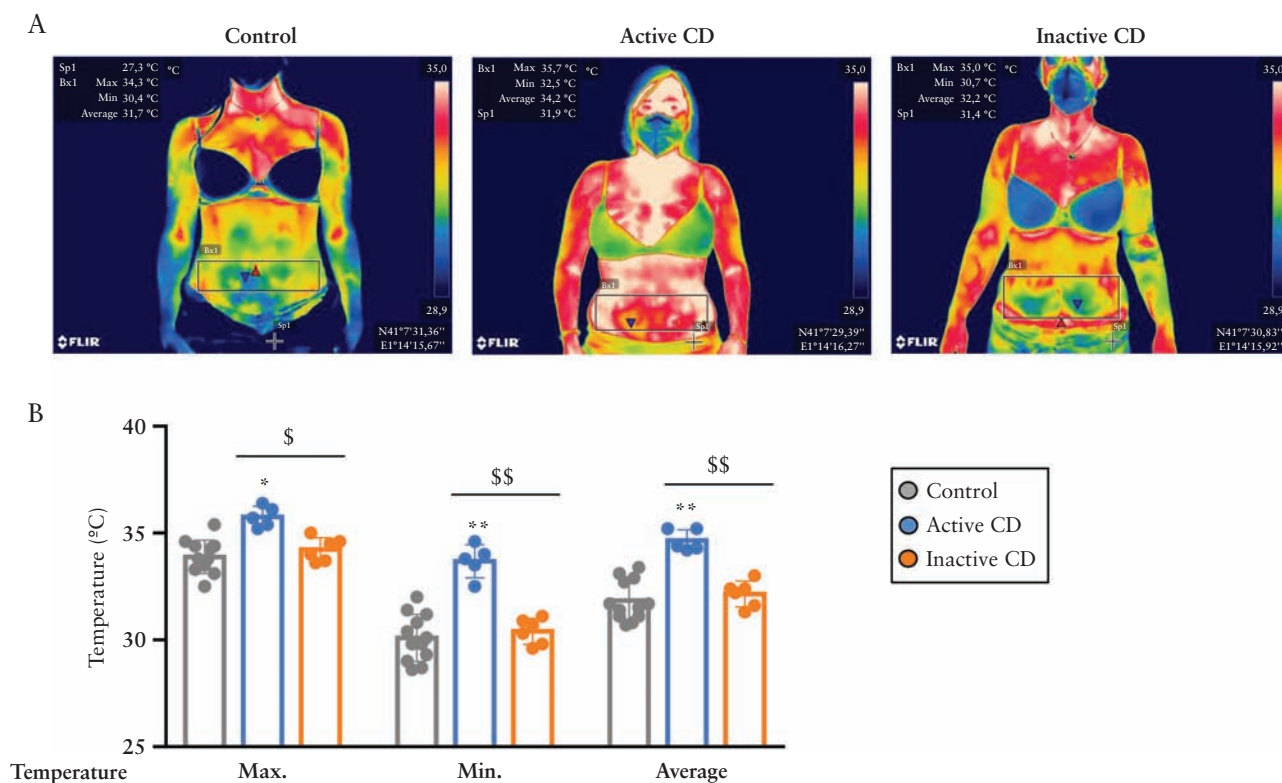


Figure 5. Abdominal temperature is elevated in patients with active Crohn's disease. [A] Representative abdominal thermal images of a healthy female, a female with inactive Crohn's disease [CD] and a female with active CD, matched by age and body mass index. [B] Maximum, minimum and average temperature of intestinal areas were obtained by selecting the area of interest with the rectangle in the FLIR tools program. The average temperature is significantly higher in active CD with respect to healthy controls and is significantly lower in inactive CD with respect to active CD. Bars in graphs represent mean \pm SEM. * $p = 0.001$; ** $p < 0.0001$ vs control; \$ $p = 0.001$ and \$\$ $p < 0.0001$ as indicated in the figure.

may have a key role in this process. Our findings also indicate that bacterial translocation might participate in ASC differentiation into beige adipocytes. These experiments have been performed in undifferentiated ASCs instead of adipocytes, which may be considered a limitation, but we have provided evidence that the changes we have observed in the ASCs [pre-adipocytes] are subsequently transferred with an increase overall in protein and gene expression of UCP1 in VAT of active CD patients.

This study has some limitations that warrant discussion. It is an observational study, with a limited number of cases, and it would be necessary to monitor the evolution of the patients across time to evaluate changes in beige adipose tissue along the clinical course and to disentangle correlation from causality regarding creeping fat and CD. Larger prospective studies will therefore be needed to decipher the clinical relevance of these findings. A limitation in the use of infrared thermography is that it may be affected by several conditions; however, we endeavoured to control several environmental, technical and individual factors. For example, patients were fasted, and room temperature, room size and distance for imaging were all controlled. Also, patients came for imaging on the same day and were matched by sex, age and BMI. A final limitation is the relatively small number of subjects included in the study, but we considered this a pilot study to be validated in future larger cohorts.

In conclusion, we provide evidence suggesting that both bacterial translocation into the creeping fat and the metabolite succinate act as activators of white AT browning in ASCs from patients with CD. This hitherto unrecognized feature of creeping fat in particular and of AT in general in CD might be exploited to develop new therapeutic or diagnostic strategies in these patients.

Funding

This study was supported by grants from the Spanish Ministry of Science and Innovation [PI18/00037 (Instituto de Salud Carlos III, ISCIII) to C.S.; PI17/01503 and PI20/00338 (ISCIII) to J.V. and RTI2018-093919 to S.F.-V.], co-financed by the European Regional Development Fund [ERDF] and a European Crohn's and Colitis Organization grant to C.S. The Spanish Biomedical Research Center in Diabetes and Associated Metabolic Disorders [CIBERDEM] [CB07708/0012] is an initiative of the Instituto de Salud Carlos III acknowledges support from the 'Ramón y Cajal' programme from the Ministerio de Educación y Ciencia [RYC2013-13186], co-financed by the ERDF. S.F.-V. acknowledge support from the 'Miguel Servet' tenure track programme [CP10/00438, CPII16/0008] from the Fondo de Investigación Sanitaria, co-financed by the ERDF. D.M.-F. acknowledges support from PERIS-PFI-Salut SLT01720000021.

Conflict of Interest

The authors have no conflicts of interest to declare.

Acknowledgments

We wish to particularly acknowledge the patients and the BioBank IISPV [PT17/0015/0029] integrated in the Spanish National Biobanks Network for its collaboration. We thank Dr Kenneth McCreath for helpful comments on the manuscript.

Author Contributions

D.M.-F., A.B.-T., C.N.-R. and C.S. performed the experiments. A.C., M.M., M.Marti, B.E., M.B. and E.E. and carried out part of the study population selection and human sample processing. J.S. performed proteomics data analysis. C.S., A.M., J.V. and S.F.-V. contributed to the discussion and reviewed the manuscript. C.S. and S.F.-V. conceived the study, discussed data and wrote the manuscript. S.F.-V. and C.S. are the guarantors of this work.

Ethics Approval

This study was approved by the ethics committee of the University Hospital Joan XXIII [CEIM 080/2021, CEIM177/2018, CEIM 41p/2015] and Hospital Vall d'Hebrón PR[CS]383/2021.

Data Availability

The accession number for the mass spectrometry proteomics data reported in this paper is ProteomeXchange: PXD030520. The other datasets generated during and/or analysed during the current study are available from the corresponding author on reasonable request.

Supplementary Data

Supplementary data are available online at ECCO-JCC online.

References

- Ha CWY, Martin A, Sepich-Poore GD, et al. Translocation of viable gut microbiota to mesenteric adipose drives formation of creeping fat in humans. *Cell* 2020;183:666–83.e17.
- Fernández-Veledo S, Vendrell J. Gut microbiota-derived succinate: friend or foe in human metabolic diseases? *Rev Endocr Metab Disord* 2019;20:439–447.
- Connors J, Dawe N, Limbergen J Van. The role of succinate in the regulation of intestinal inflammation. *Nutrients* 2019;11:25.
- Ortiz-Masiá D, Gisbert-Ferrándiz L, Bauset C, et al. Succinate activates EMT in intestinal epithelial cells through SUCNR1: a novel protagonist in fistula development. *Cells* 2020;9:1104.
- Fremder M, Kim SW, Khamaysi A, et al. A transepithelial pathway delivers succinate to macrophages, thus perpetuating their pro-inflammatory metabolic state. *Cell Rep* 2021;36:109521.
- Chouchani ET, Pell VR, Gaude E, et al. Ischaemic accumulation of succinate controls reperfusion injury through mitochondrial ROS. *Nature* 2014;515:431–5.
- Littlewood-Evans A, Sarret S, Apfel V, et al. GPR91 senses extracellular succinate released from inflammatory macrophages and exacerbates rheumatoid arthritis. *J Exp Med* 2016;213:1655–62.
- Rubic T, Lametschwandtner G, Jost S, et al. Triggering the succinate receptor GPR91 on dendritic cells enhances immunity. *Nat Immunol* 2008;9:1261–9.
- Tannahill GM, Curtis AM, Adamik J, et al. Succinate is an inflammatory signal that induces IL-1 β through HIF-1 α . *Nature* 2013;496:238–42.
- Keiran N, Ceperuelo-Mallafré V, Calvo E, et al. SUCNR1 controls an anti-inflammatory program in macrophages to regulate the metabolic response to obesity. *Nat Immunol* 2019;20:581–92.
- Lei W, Ren W, Ohmoto M, et al. Activation of intestinal tuft cell-expressed *sucnr1* triggers type 2 immunity in the mouse small intestine. *Proc Natl Acad Sci U S A* 2018;115:5552–7.
- Nadjsombati MS, McGinty JW, Lyons-Cohen MR, et al. Detection of succinate by intestinal tuft cells triggers a type 2 innate immune circuit. *Immunity* 2018;49:33–41.e7.
- Peruzzotti-Jametti L, Bernstock JD, Vicario N, et al. Macrophage-derived extracellular succinate licenses neural stem cells to suppress chronic neuroinflammation. *Cell Stem Cell* 2018;22:355–68.e13.
- Mills EL, Pierce KA, Jedrychowski MP, et al. Accumulation of succinate controls activation of adipose tissue thermogenesis. *Nature* 2018;560:102–6.
- Mills EL, Harmon C, Jedrychowski MP, et al. UCP1 governs liver extracellular succinate and inflammatory pathogenesis. *Nat Metab* 2021;3:604–17.
- Liu K, Lin L, Li Q, et al. *Scd1* controls de novo beige fat biogenesis through succinate-dependent regulation of mitochondrial complex II. *Proc Natl Acad Sci U S A* 2020;117:2462–72.
- Han SJ, Glatman Zaretsky A, Andrade-Oliveira V, et al. White adipose tissue is a reservoir for memory T cells and promotes protective memory responses to infection. *Immunity* 2017;47:1154–68.e6.
- Munro P, Rekima S, Loubat A, et al. Impact of thermogenesis induced by chronic β 3-adrenergic receptor agonist treatment on inflammatory and infectious response during bacteremia in mice. *PLoS One* 2021;16:e0256768.
- Ayalon I, Shen H, Williamson L, et al. Sepsis induces adipose tissue browning in nonobese mice but not in obese mice. *Shock* 2018;50:557–64.
- Ayari A, Rosa-Calatrava M, Lancel S, et al. Influenza infection rewires energy metabolism and induces browning features in adipose cells and tissues. *Commun Biol* 2020;3:1–15.
- Johanna Barthelemy IW. Influenza A virus infection induces white adipose tissue browning: a metabolic adaptation to infection? *J Cell Immunol* 2020;3:237.
- Best WR, Bechtel JM, Singleton JW, et al. Development of a Crohn's disease Activity Index: National Cooperative Crohn's Disease Study. *Gastroenterology* 1976;70:439–44.
- Assche G Van, Dignass A, Reinisch W, et al. The second European evidence-based Consensus on the diagnosis and management of Crohn's disease: special situations. *J Crohns Colitis* 2010;4:63–101.
- Serena C, Keiran N, Madeira A, et al. Crohn's disease disturbs the immune properties of human adipose-derived stem cells related to inflammasome activation. *Stem Cell Reports* 2017;9:1109–23.
- Serena C, Millan M, Ejarque M, et al. Adipose stem cells from patients with Crohn's disease show a distinctive DNA methylation pattern. *Clin Epigenetics* 2020;12:53.
- Pachón-Peña G, Yu G, Tucker A, et al. Stromal stem cells from adipose tissue and bone marrow of age-matched female donors display distinct immunophenotypic profiles. *J Cell Physiol* 2011;226:843–51.
- Ceperuelo-Mallafré V, Ejarque M, Serena C, et al. Adipose tissue glycogen accumulation is associated with obesity-linked inflammation in humans. *Mol Metab* 2016;5:5–18.
- Serena C, Keiran N, Ceperuelo-Mallafré V, et al. Obesity and type 2 diabetes alters the immune properties of human adipose derived stem cells. *Stem Cells* 2016;34:2559–73.
- Titos E, Rius B, González-Pérez A, et al. Resolvin D1 and its precursor docosahexaenoic acid promote resolution of adipose tissue inflammation by eliciting macrophage polarization toward an M2-like phenotype. *J Immunol* 2011;187:5408–18.
- Pachón-Peña G, Serena C, Ejarque M, et al. Obesity determines the immunophenotypic profile and functional characteristics of human mesenchymal stem cells from adipose tissue. *Stem Cells Transl Med* 2016;5:464–75.
- Astiarraga B, Martínez L, Ceperuelo-Mallafré V, et al. Impaired succinate response to a mixed meal in obesity and type 2 diabetes is normalized after metabolic surgery. *Diabetes Care* 2020;43:2581–7.
- Serena C, Ceperuelo-Mallafré V, Keiran N, et al. Elevated circulating levels of succinate in human obesity are linked to specific gut microbiota. *ISME J* 2018;12:1642–57.

33. Fernández-Cuevas I, Bouzas Marins JC, Arnáiz Lastras J, *et al.* Classification of factors influencing the use of infrared thermography in humans: a review. *Infrared Phys Technol* 2015;71:28–55.
34. Kyle UG, Bosaeus I, Lorenzo AD De, *et al.* Bioelectrical impedance analysis - Part I: review of principles and methods. *Clin Nutr* 2004;23:1226–43.
35. Macias-Ceja DC, Ortiz-Masiá D, Salvador P, *et al.* Succinate receptor mediates intestinal inflammation and fibrosis. *Mucosal Immunol* 2019;12:178–87.
36. Gilissen J, Jouret F, Pirotte B, *et al.* Insight into SUCNR1 (GPR91) structure and function. *Pharmacol Ther* 2016;159:56–65.
37. Villarroja J, Cereijo R, Giralt M, *et al.* Secretory proteome of brown adipocytes in response to cAMP-mediated thermogenic activation. *Front Physiol* 2019;10:1–8.
38. Li J, Li J, Zhao WG, *et al.* Comprehensive proteomics and functional annotation of mouse brown adipose tissue. *PLoS One* 2020;15:1–16.
39. Müller S, Balaz M, Stefanicka P, *et al.* Proteomic analysis of human brown adipose tissue reveals utilization of coupled and uncoupled energy expenditure pathways. *Sci Rep* 2016;6:1–9.
40. Graja A, Garcia-Carrizo F, Jank AM, *et al.* Loss of periostin occurs in aging adipose tissue of mice and its genetic ablation impairs adipose tissue lipid metabolism. *Aging Cell* 2018;17:e12810.
41. Braga M, Reddy ST, Vergnes L, *et al.* Follistatin promotes adipocyte differentiation, browning, and energy metabolism. *J Lipid Res* 2014;55:375–84.
42. Hampton M, Melvin RG, Andrews MT. Transcriptomic analysis of brown adipose tissue across the physiological extremes of natural hibernation. *PLoS One* 2013;8:1–12.
43. Duclos S, Diez R, Garin J, *et al.* Rab5 regulates the kiss and run fusion between phagosomes and endosomes and the acquisition of phagosome leishmanicidal properties in RAW 264.7 macrophages. *J Cell Sci* 2000;113:3531–41.
44. Cioffi I, Marra M, Imperatore N, *et al.* Assessment of bioelectrical phase angle as a predictor of nutritional status in patients with Crohn's disease: a cross sectional study. *Clin Nutr* 2020;39:1564–71.
45. Langenberg DR Van, Della GP, Hill B, *et al.* Delving into disability in Crohn's disease: dysregulation of molecular pathways may explain skeletal muscle loss in Crohn's disease. *J Crohns Colitis* 2014;8:626–34.
46. Kredel LI, Siegmund B. Adipose-tissue and intestinal inflammation - visceral obesity and creeping fat. *Front Immunol* 2014;5:462.
47. Zulian A, Canello R, Micheletto G, *et al.* Visceral adipocytes: old actors in obesity and new protagonists in Crohn's disease? *Gut* 2012;61:86–94.
48. Omran F, Christian M. Inflammatory signaling and brown fat activity. *Front Endocrinol* 2020;11:156.
49. Pervin S, Singh V, Tucker A, *et al.* Modulation of transforming growth factor- β /follistatin signaling and white adipose browning: therapeutic implications for obesity related disorders. *Horm Mol Biol Clin Investig* 2017;31.
50. Lee P, Werner CD, Kebebew E, *et al.* Functional thermogenic beige adipogenesis is inducible in human neck fat. *Int J Obes* 2014;38:170–6.
51. Rahman S, Lu Y, Czernik PJ, *et al.* Inducible brown adipose tissue, or beige fat, is anabolic for the skeleton. *Endocrinology* 2013;154:2687–701.
52. Holmes D. Epigenetics: on-off switch for obesity. *Nat Rev Endocrinol* 2016;12:125.
53. Kajimura S. Engineering fat cell fate to fight obesity and metabolic diseases. *Keio J Med* 2015;64:65.
54. Li S, Gao H, Hasegawa Y, *et al.* Fight against fibrosis in adipose tissue remodeling. *Am J Physiol - Endocrinol Metab* 2021;321:E169–75.
55. Curciarello R, Docena GH, MacDonald TT. The role of cytokines in the fibrotic responses in Crohn's disease. *Front Med* 2017;4:126.
56. Carino A, Cipriani S, Marchianò S, *et al.* BAR502, a dual FXR and GPBAR1 agonist, promotes browning of white adipose tissue and reverses liver steatosis and fibrosis. *Sci Rep* 2017;7:1–13.
57. Serena C, Queipo-Ortuño M, Millan M, *et al.* Microbial signature in adipose tissue of Crohn's disease patients. *J Clin Med* 2020;9:2448.